

An analytical approach to migration velocity analysis

Zhenyue Liu*

ABSTRACT

Prestack depth migration provides a powerful tool for velocity analysis in complex media. Both prominent approaches to velocity analysis—depth-focusing analysis and residual-curvature analysis, rely on approximate formulas to update velocity. Generally, these formulas are derived under the assumptions of horizontal reflector, lateral velocity homogeneity, or small offset. Therefore, the conventional methods for updating velocity lack accuracy and computational efficiency when velocity has large, lateral variations.

Here, based on ray theory, I find the analytic representation for the derivative of imaged depths with respect to migration velocity. This derivative function characterizes a general relationship between residual moveout and residual velocity. Using the derivative function and the perturbation method, I derive a new formula to update velocity from residual moveout. In the derivation, I impose no limitation on offset, dip, or velocity distribution. Consequently, I revise the residual-curvature-analysis method for velocity estimation in the postmigrated domain. Furthermore, my formula provides sensitivity and error estimation for migration-based velocity analysis, which is helpful in quantifying the reliability of the estimated velocity.

The theory and methodology in this paper have been tested on synthetic data (including the Marmousi data).

INTRODUCTION

Prestack depth migration that can handle dipping reflectors and lateral velocity variations is robust in imaging complex structures. To process data by this method, one often needs to have a more accurate velocity model than may be obtained from simple velocity-analysis methods, such as normal moveout. Meanwhile, prestack depth migration itself is an attractive tool for doing velocity analysis because of its high sensitivity

to the velocity model. Two approaches to migration velocity analysis have been developed: depth-focusing analysis (DFA) and residual-curvature analysis (RCA). Depth-focusing analysis is based on using stacking power to measure velocity error. Residual-curvature analysis is based on residual moveout to measure velocity error.

Migration velocity analysis must address two issues to succeed: (1) how to establish a criterion for knowing if a migration velocity is acceptable, and (2) how to update the velocity, if it is unacceptable. In DFA, a migration velocity is acceptable if the difference between migration depth and focusing depth is zero. In RCA, a migration velocity is acceptable if the difference between imaged depths from different offsets is zero. Quantitatively, these differences can be used to update the velocity in a routine way. To date, a variety of updating formulas have been developed. These formulas degrade with increasing complexity of media (lateral velocity variation and reflector dip), because of rough approximations used to estimate velocity. Although iteration generally is helpful in obtaining a more accurate velocity, a good approximation not only reduces the number of iterations but also increases the likelihood of the convergence. The conventional formulas for updating velocity were derived under one or more assumptions as follows:

- 1) lateral velocity homogeneity,
- 2) small offset, or
- 3) horizontal reflector.

In MacKay and Abma's (1992) DFA approach, all three assumptions are used. In RCA, the assumptions vary with migration types. For common-shot migration or common-receiver migration, Al-Yahya's (1989) formula used all three assumptions. Lee and Zhang (1992) derived a formula that replaces assumption (3) by the assumption of small dip. For common-offset migration, Deregowski's (1990) formula used the first two assumptions. [This statement was varified by Liu and Bleistein (1992).] Both DFA and RCA use assumptions (1) and (2). Under the assumption of a small offset, the residual moveout can be approximated by a hyperbola or a parabola.

Manuscript received by the Editor August 11, 1995; revised manuscript received July 29, 1996.

*Formerly Center for Wave Phenomena, Colorado School of Mines, Golden, Colorado 80401; presently Exxon Production Research Company, 3616 Richmond Avenue, Houston, Texas 77046.

© 1997 Society of Exploration Geophysicists. All rights reserved.

However, this approximation is poor when the velocity has strong lateral variation.

Conventional approaches to updating the velocity inspect information at each midpoint individually. This information is not reliable when conflicting events exist because velocity estimation will depend on which event is used. Furthermore, the conventional approaches update the average velocities that are assumed to be equal to the rms velocities and then convert rms velocities into interval velocities by the Dix equation or other methods. Unfortunately, when the velocity has a lateral anomaly, this kind of average velocity may differ significantly from the rms velocity (Toldi, 1989), which may cause divergence in the velocity-updating procedure.

Because of such limitations, conventional approaches to velocity analysis encounter difficulties in handling complex structures (such as the Marmousi model). To overcome these limitations, some geophysicists used a macro-model (layer-stripping) method for estimating the interval velocity directly. A macro-model consists of velocities and velocity interfaces (subsurfaces). The model is determined by layer-stripping in a top down procedure. Then the velocity of each layer is updated iteratively by using depth-focusing analysis or residual-curvature analysis; and the velocity interface is imaged by using the corrected velocity. The whole process may be accomplished with interpretation based on geological knowledge. So far, the present macro-model method has two significant drawbacks. First, the velocity distribution is assumed to be constant in layers. In fact, velocity may vary within a layer. Second, there has not been a systematic formula for updating velocity, which results in inaccuracy and inefficiency for velocity estimates.

In this paper, I present a new approach to migration velocity analysis that revises the RCA method. Based on ray theory, migration processes can be kinematically described by the so-called imaging equations (Liu and Bleistein, 1995). From these imaging equations, I find the representation for the derivative of imaged depths with respect to migration velocity. This derivative function characterizes a general relationship between residual moveout and residual velocity. Using the derivative function and the perturbation method, I derive a new formula to update velocity from residual moveout. Significantly different from conventional ones, my formula is valid for any offset, dip, and velocity distribution. A similar formula was proposed in Lafond and Levander (1993). However, that formula is restricted to constant-velocity layers. In contrast, my formula can handle any parameterization of velocity.

The idea of using perturbation is suggested by tomography approaches to velocity estimation. Under the assumption of small velocity perturbation, there is a linear relationship between the residual traveltimes and the residual velocity. In the tomographic approach, raypaths are required to construct the equation system for velocity estimation. However, raypath construction seems more difficult in reflection tomography than in refraction tomography. Raypaths depend strongly on the reflector position (depth and slope) in reflection tomography. Although the depths can be included in the inverse problem as parameters to be determined (Stork and Clayton, 1991), generally it is difficult to determine the slope's accurately. In contrast, here I use the stationary-phase principle to determine specular raypaths, without requiring knowledge of an accurate reflector position. This is the same technique as

was used to determine the normal raypath incidence angle in Kirchhoff inversion [see Bleisten et al. (1987)].

Although prestack migration has advantages when dealing with complex media, its weaknesses should be considered in application. Besides its high cost, complexity of medium may degrade the effectiveness of the prestack migration method. Here, I discuss the sensitivity of migration-based velocity analysis, and show what factors affect the sensitivity, so that I may estimate the velocity error involved in the velocity analysis. Furthermore, this sensitivity analysis provides an indicator of when a priori geological knowledge is necessary for estimating reasonable velocities.

FORMULATION OF VELOCITY ESTIMATE

With no loss of generality, I assume that the datum surface is flat. Let x_s be the source position and x_r be the receiver position on the surface. For any point (x, z) below the surface, $\tau_s(x_s; x, z)$ or $\tau_r(x, z; x_r)$, respectively, denote traveltimes from x_s to (x, z) , or (x, z) to x_r .

Suppose I know the total reflection travetime function $t(y, h)$ (therefore, $\partial t/\partial y$) that depends on midpoint y and half-offset h . Given a velocity function $v(x, z)$, then, for each h , the reflector is determined by

$$\tau_s(x_s; x, z) + \tau_r(x, z; x_r) = t(y, h), \quad (1)$$

$$\frac{\partial \tau_s}{\partial y} + \frac{\partial \tau_r}{\partial y} = \frac{\partial t}{\partial y}. \quad (2)$$

In a common image gather, the imaged depth z can be determined as a function of h . If the migration velocity equals the true velocity, then the imaged depth z will be independent of offset h ; otherwise—for incorrect velocity— z varies with offset h . Consequently, the imaged depths in common image gathers (CIGs) provide information on the velocity distribution.

Equations (1) and (2) are valid even if the migration velocity is wrong. The dependency of traveltimes on velocity in equations (1) and (2) implies that this equation system displays a general relationship between the imaged depth and migration velocity. However, this equation system is nonlinear, making it difficult to solve directly for velocity. Here, I use a mathematical tool—perturbation—to linearize this equation system by considering perturbations in model parameters. Before the perturbation is applied, I need to describe the velocity as a function of parameters and to compute the derivative of imaged depths with respect to those parameters.

Suppose that the velocity distribution v is characterized by a parameter or a family of parameters λ ,

$$v = v(x, z; \lambda). \quad (3)$$

For example, when $v(x, z; \lambda) = v_0 + ax + bz$, λ is any set of one to three parameters chosen from v_0 , a , and b . Thus, the problem of velocity estimation becomes a problem of parameter estimation. The relationship between the imaged depths and a velocity distribution is determined by the derivative function,

$$g(x, h) = \frac{dz}{d\lambda}. \quad (4)$$

The expression, g , will be derived from equations (1) and (2). To simplify the derivation, I suppose that λ is just a single parameter at first.

For a fixed image location x and a fixed offset (common-offset case), I differentiate equation (1) with respect to λ . Note that y and z are functions of λ ; then

$$\begin{aligned} & \left[\frac{\partial \tau_s}{\partial y} + \frac{\partial \tau_r}{\partial y} \right] \frac{dy}{d\lambda} + \left[\frac{\partial \tau_s}{\partial \lambda} + \frac{\partial \tau_r}{\partial \lambda} \right] \\ & + \left[\frac{\partial \tau_s}{\partial z} + \frac{\partial \tau_r}{\partial z} \right] \frac{dz}{d\lambda} = \frac{\partial t}{\partial y} \frac{dy}{d\lambda}. \end{aligned} \quad (5)$$

By using equation (2), the first term on the left side of equation (5) is balanced by the right-hand term. Therefore,

$$\left[\frac{\partial \tau_s}{\partial z} + \frac{\partial \tau_r}{\partial z} \right] \frac{dz}{d\lambda} = -\frac{\partial \tau_s}{\partial \lambda} - \frac{\partial \tau_r}{\partial \lambda}. \quad (6)$$

Let θ_s or θ_r be the angle between the raypath from the source or the receiver, and the vertical at (x, z) ; then

$$\frac{\partial \tau_s}{\partial z} = \frac{\cos \theta_s}{v(x, z; \lambda)}, \quad \frac{\partial \tau_r}{\partial z} = \frac{\cos \theta_r}{v(x, z; \lambda)}. \quad (7)$$

Using this result, equation (6) is rewritten as

$$\frac{\cos \theta_s + \cos \theta_r}{v(x, z; \lambda)} \frac{dz}{d\lambda} = -\frac{\partial \tau_s}{\partial \lambda} - \frac{\partial \tau_r}{\partial \lambda}. \quad (8)$$

Thus the derivative of imaged depth with respect to λ is found by

$$g(x, h) = -\left[\frac{\partial \tau_s}{\partial \lambda} + \frac{\partial \tau_r}{\partial \lambda} \right] \frac{v(x, z; \lambda)}{\cos \theta_s + \cos \theta_r}. \quad (9)$$

The function g characterizes the relationship between the imaged depth and the migration velocity in a general medium context. The computation of this function will result in a new velocity analysis method, compared to conventional ones based on the assumption of hyperbolic residual moveout.

Suppose that the true parameter is λ^* and the true reflection depth is z^* . If there is a small perturbation $\delta\lambda = \lambda^* - \lambda$ between the true parameter and the parameter used in migration, then the imaged depth will have a corresponding perturbation

$$\delta z(x, h) \equiv z^* - z(x, h) \approx \frac{dz}{d\lambda} \delta\lambda. \quad (10)$$

By using equation (4), a linearized equation is set for $\delta\lambda$ as

$$\delta z = g(x, h) \delta\lambda. \quad (11)$$

Equation (11) is valid for an arbitrary velocity distribution, arbitrary reflector dips, and any offset, as long as the velocity perturbation is sufficiently small, which is significantly different from the limited result of conventional RCA.

Remark. When the velocity distribution is constant in layers, one can take λ as the velocity v itself in the target layer. In this situation,

$$\frac{\partial \tau_s}{\partial \lambda} + \frac{\partial \tau_r}{\partial \lambda} = -\frac{t_s + t_r}{v}, \quad (12)$$

where t_s (or t_r) is a partial traveltime of τ_s (or τ_r) within this layer. Thus, the derivative function g is simplified to

$$g(x, h) = \frac{t_s + t_r}{\cos \theta_s + \cos \theta_r}. \quad (13)$$

This typical result was obtained by Lafond and Levander (1993).

When the velocity distribution is characterized by multiple parameters, $\hat{\lambda} = (\lambda_1, \lambda_2, \dots, \lambda_n)^T$, the imaged-depth perturbation will depend on the perturbations of all these parameters. Therefore, equation (11) will be modified by

$$\delta z(x, h) = \sum_{i=1}^n \frac{\partial z}{\partial \lambda_i} \delta \lambda_i = \sum_{i=1}^n g_i(x, h) \delta \lambda_i, \quad (14)$$

where each derivative function is calculated by

$$g_i(x, h) = -\left[\frac{\partial \tau_s}{\partial \lambda_i} + \frac{\partial \tau_r}{\partial \lambda_i} \right] \frac{v(x, z; \hat{\lambda})}{\cos \theta_s + \cos \theta_r}. \quad (15)$$

If one could solve for $\delta \hat{\lambda}$, the true parameters can be estimated by

$$\hat{\lambda}^* = \hat{\lambda} + \delta \hat{\lambda}. \quad (16)$$

Notice that the left side of equation (14) involves the true depth z^* that is unknown. Conventional methods deal with this problem by using the concept of the reference depth (Lafond and Levander, 1993) or adding z^* as a new unknown (Stork and Clayton, 1991). Here, I use a technique in equation (14) to remove z^* directly. The true depth can be approximately replaced by the corrected imaged depth $z + \delta z$,

$$z^* \approx z(x, h) + \delta z(x, h) = z(x, h) + \sum_{i=1}^n g_i(x, h) \delta \lambda_i. \quad (17)$$

The true reflection depth z^* is independent of offset. Therefore, the corrected imaged depths from different offsets should be close to each other. Mathematically, this statement means that the variance of these depths is a minimum. Suppose that there are offsets h_1, h_2, \dots, h_m , and image locations x_1, x_2, \dots, x_K ; then

$$z_j^{(k)} + \delta z_j^{(k)} = z_j^{(k)} + \sum_{i=1}^n g_{ij}^{(k)} \delta \lambda_i, \quad (18)$$

where

$$z_j^{(k)} = z(x_k, h_j), \quad \delta z_j^{(k)} = \delta z(x_k, h_j), \quad g_{ij}^{(k)} = g_i(x_k, h_j). \quad (19)$$

I seek $\delta \lambda_i$'s such that the corrected imaged depths have the minimum variance; i.e.,

$$\sum_{k=1}^K \sum_{j=1}^m \left(z_j^{(k)} + \delta z_j^{(k)} - \overline{\hat{z}^{(k)}} + \delta \hat{z}^{(k)} \right)^2 = \min, \quad (20)$$

where

$$\hat{z}^{(k)} = \left(z_1^{(k)}, z_2^{(k)}, \dots, z_m^{(k)} \right)^T, \quad (21)$$

and

$$\delta \hat{z}^{(k)} = \left(\delta z_1^{(k)}, \delta z_2^{(k)}, \dots, \delta z_m^{(k)} \right)^T. \quad (22)$$

Here, I use the overline to denote the mean value of a vector over the offset index. For example,

$$\overline{\hat{z}^{(k)}} = \frac{1}{m} \sum_{j=1}^m z_j^{(k)}. \quad (23)$$

Introduce the matrix and vector,

$$A^{(k)} \equiv \left[a_{i\ell}^{(k)} \right]_{n \times n}, \quad \hat{b}^{(k)} \equiv \left(b_1^{(k)}, b_2^{(k)}, \dots, b_n^{(k)} \right)^T, \quad (24)$$

where

$$a_{i\ell}^{(k)} = \sum_{j=1}^m \left(g_{ij}^{(k)} - \overline{\hat{g}_i^{(k)}} \right) \left(g_{\ell j}^{(k)} - \overline{\hat{g}_\ell^{(k)}} \right), \quad (25)$$

$$b_i^{(k)} = \sum_{j=1}^m \left(g_{ij}^{(k)} - \overline{\hat{g}_i^{(k)}} \right) \left(z_j^{(k)} - \overline{\hat{z}^{(k)}} \right), \quad (26)$$

and

$$\hat{g}_i^{(k)} = \left(g_{i1}^{(k)}, g_{i2}^{(k)}, \dots, g_{in}^{(k)} \right)^T; \quad (27)$$

then, as shown in Appendix A, the solution of minimization (20) must satisfy the linear equation,

$$\left[\sum_{k=1}^K A^{(k)} \right] \delta \hat{\lambda} = - \sum_{k=1}^K \hat{b}^{(k)}. \quad (28)$$

Specifically, if there is only one velocity parameter to be determined, i.e., $n = 1$, then equation (28) will have an explicit solution

$$\delta \lambda = - \frac{\sum_{k=1}^K \sum_{j=1}^m \left(g_j^{(k)} - \overline{\hat{g}^{(k)}} \right) \left(z_j^{(k)} - \overline{\hat{z}^{(k)}} \right)}{\sum_{k=1}^K \sum_{j=1}^m \left(g_j^{(k)} - \overline{\hat{g}^{(k)}} \right)^2}, \quad (29)$$

where the index on the velocity parameter is omitted since $n = 1$.

If the corrected imaged depths are not close enough to each other, I implement iteration to obtain more accurate parameters. The iteration stops where the variance (20) achieves a given sufficiently small value.

COMPUTATIONAL TECHNIQUES

Calculation of the derivative function

The function $g(x, h)$ in equation (9) involves the derivatives of traveltimes with respect to the parameter λ . In the eikonal equation,

$$\left(\frac{\partial \tau}{\partial x} \right)^2 + \left(\frac{\partial \tau}{\partial z} \right)^2 = \frac{1}{v^2(x, z; \lambda)}. \quad (30)$$

Differentiating here with respect to λ yields

$$\frac{\partial \mu}{\partial x} \frac{\partial \tau}{\partial x} + \frac{\partial \mu}{\partial z} \frac{\partial \tau}{\partial z} = \frac{1}{2} \frac{\partial}{\partial \lambda} \left(\frac{1}{v^2(x, z; \lambda)} \right), \quad (31)$$

where $\mu = \partial \tau / \partial \tau$. The integral solution of equation (31) is

$$\mu = \int_L \frac{\partial}{\partial \lambda} \left(\frac{1}{v(x, z; \lambda)} \right) dL, \quad (32)$$

where L is the raypath from the source (or receiver) to the image point (x, z) .

For each source or receiver, $\partial \tau / \partial \lambda$ can be determined from equation (31) or (32). Therefore, given an image point (x, z) and a specular source–receiver pair x_s and x_r , one can calculate g from equation (9). However, there is not an explicit formula to represent the specular source–receiver pair from the image

point for a complex medium. To solve this problem, here, I use the Kirchhoff integral to calculate g . In the Kirchhoff summation, I calculate two migration outputs that have the same phase but different amplitudes. One uses the original amplitude; the other one uses the original amplitude multiplied by the quantity g . Thus, the ratio of the amplitudes of these two outputs will evaluate g at the specular source–receiver position according to the stationary-phase principle, without requiring knowledge of the specular source–receiver pair. This technique is the same as was used to determine the normal incidence angle in Kirchhoff inversion (Bleistein et al., 1987). The accuracy of calculating the derivative function g depends on the S/N ratio in seismic data and the power of stationary phase method.

Parameterization of velocity distribution

Although equation (28) holds for any velocity distribution, the solution will be underdetermined and unstable if too many unknown parameters are involved. Consequently, it is essential to characterize the velocity distribution by choosing appropriate parameters. Conventionally, one assumes that a velocity model consists of the construction of the macro-model (constant velocities and velocity interfaces). The interfaces divide the whole model into a number of blocks (shown in Figure 1). Here, I replace constant velocity in one block by a linear function that is characterized by three parameters:

$$\lambda_1 + \lambda_2(z - z_0) + \lambda_3(x - x_0), \quad (33)$$

where (x_0, z_0) is a reference point. Thus, the velocity distribution is written in a form

$$v(x, z) = v_0(x, z) + \lambda_1 + \lambda_2(z - z_0) + \lambda_3(x - x_0), \quad (34)$$

where v_0 is a background velocity.

An imaged depth only depends on the velocity above it, except for turning rays. Therefore, use of a recursive algorithm (layer stripping) is possible to determine velocity in an individual block. I start from the block nearest surface. For example, I choose the top left block in Figure 1. In each block, iteration is used to calculate velocity parameters. Given an initial guess for λ_i 's, common-offset depth migration is implemented to obtain imaged depths and $g_i(x, h)$ in equation (15) for common-image gathers. Equation (28) will give a correction of the λ_i 's; then

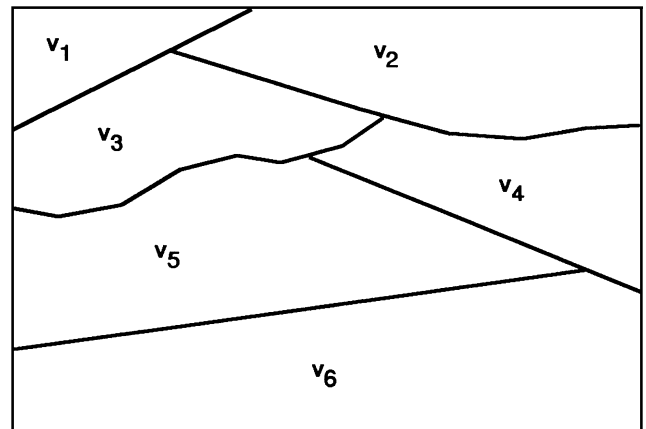


FIG. 1. Macro model.

using the updated parameters as a new initial guess, I correct the velocity again until the convergence is achieved. After velocity analysis in one block, I migrate data with the corrected velocity, and pick the velocity interface from the imaged structure. When I finish determining the velocity and velocity interface in one block, I will repeat the same procedure in the next block that is located below the finished block.

SENSITIVITY OF MIGRATION VELOCITY ANALYSIS

Velocity analysis by prestack migration uses the discrepancy between the imaged depths from different offsets, which is represented by equation (28), to correct the velocities. If the variance defined by equation (20) is zero, one can conclude that the velocity is correct. However, it is impractical to obtain an exact zero variance. There are many factors against achieving this goal: noise in the input data, nonacoustic properties, inaccurate description of velocity distribution, and so on. Even if an apparent zero variance is obtained, the actual one may not be zero because of the errors involved in picking the imaged depths. Therefore, it is helpful if one can estimate how much error of migration velocity analysis is caused by the position error in imaged depths.

Quantitatively, the matrices in equation (28) that depend on the functions g_i , can be used to describe the sensitivity of the velocity error $\delta\lambda$, to the variance of residual-moveout error. Here, I will derive analytical representations for a simple case.

Suppose that the velocity $v(x, z)$ consists of a constant background velocity v_0 and a perturbation that is a linear function of depth in one block. Moreover, I assume that the upper boundary of the block is a horizontal line, $z = d$, and the reflector, located at $z = z^*$, is the bottom boundary of this block. The velocity function can be represented by

$$v(x, z) = v_0 + \alpha(\lambda_1 + \lambda_2(z - z_0)), \quad (35)$$

where $\alpha = 0$ for $z < d$, $\alpha = 1$ for $z > d$, and z_0 is a reference depth (not necessarily in the block). A sketch for this block is shown in Figure 2.

The initial guesses are set to $\lambda_1 = \lambda_2 = 0$. As shown in Appendix B, I obtain the following representation for the g_i 's that

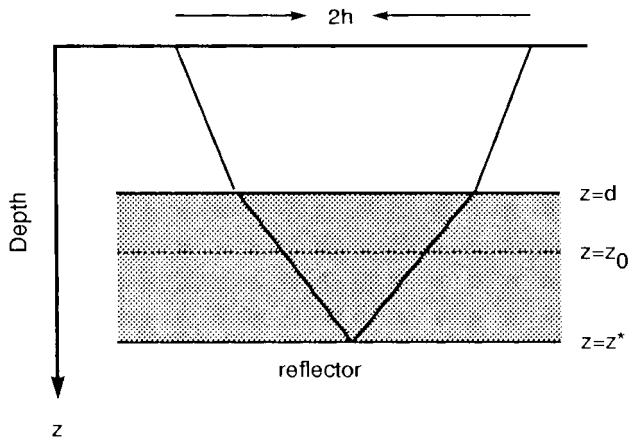


FIG. 2. Layer model. The gray shading denotes the target layer for velocity analysis.

are defined in equation (15),

$$g_1(x, h) = \frac{h^2 + z^2}{z^2} \frac{z - d}{v_0}, \quad (36)$$

$$g_2(x, h) = \frac{h^2 + z^2}{z^2} \frac{(z - z_0)^2 - (d - z_0)^2}{2v_0}. \quad (37)$$

From the above two equations, I have

$$g_2(x, h) = \frac{(z - z_0)^2 - (d - z_0)^2}{2(z - d)} g_1(x, h). \quad (38)$$

This means that the coefficients g_1 and g_2 in equation (14) are proportional for all image locations and all offsets, so that one cannot solve for λ_1 and λ_2 independently. Thus, I arrive at following conclusion: *The parameters λ_1 and λ_2 cannot be determined simultaneously if only one reflector segment is used in the velocity-analysis process. In other words, reflection information from one depth only allows to determine one parameter in the depth direction.*

This conclusion shows that one should avoid solving for λ_1 and λ_2 at the same time unless well-separated reflector segments in the depth direction are used for velocity analysis.

If the parameter λ_2 is given (i.e., $\delta\lambda_2 = 0$), then equation (14) is simplified to

$$\delta z(x, h) = \left(\frac{h^2}{z^2} + 1 \right) \frac{z - d}{v_0} \delta\lambda_1. \quad (39)$$

When $\delta\lambda_1$ is small, $z(x, h) \approx z^*$. Therefore, for the given two offsets h_2 and h_1 ($h_2 > h_1$), the difference of imaged depths from these two offsets is

$$z(x, h_2) - z(x, h_1) = \frac{(h_2^2 - h_1^2)(z^* - d)}{(z^*)^2 v_0} \delta\lambda_1. \quad (40)$$

The above equation shows that *the error in λ_1 is inversely proportional to the thickness of the block layer*. When there is a thin layer, the velocity estimation for this layer is often unreliable, so I conclude that migration-based velocity analysis cannot handle thin layers.

Similarly, if the parameter λ_1 is given (i.e., $\delta\lambda_1 = 0$), then

$$z(x, h_2) - z(x, h_1) = \frac{(h_2^2 - h_1^2)(z^* - d)(z^* + d - 2z_0)}{2(z^*)^2 v_0} \delta\lambda_2. \quad (41)$$

The above equation shows that *the error in λ_2 is determined not only by the thickness of the block layer but also by $(z^* + d)/2 - z_0$ —the difference between the central depth of the block layer and the reference depth z_0* . From equation (41), it seems likely that the estimate of λ_2 depends on the reference depth z_0 . However, by using equation (41), the average velocity in this block will be

$$v_0 + 0.5(z^* + d - 2z_0) \delta\lambda_2 = v_0 \left[1 + \frac{(z^*)^2}{(h_2^2 - h_1^2)(z^* - d)} \right], \quad (42)$$

which is independent of z_0 .

For a general case, it is difficult to obtain analytical representations for the g_i 's. However, I can calculate the g_i 's numerically, as described above, and use these values to estimate the velocity error. Specifically, if there is only one parameter,

equation (29) gives a direct error estimation,

$$|\delta\lambda| \leq \left[\frac{\sum_{k=1}^K \sum_{j=1}^m (\hat{z}_j^{(k)} - \bar{z}^{(k)})^2}{\sum_{k=1}^K \sum_{j=1}^m (g_j^{(k)} - \bar{g}^{(k)})^2} \right]^{1/2}, \quad (43)$$

where the Cauchy-Schwarz inequality has been used.

COMPUTER IMPLEMENTATION

To demonstrate the effectiveness and the efficiency of the velocity analysis techniques above, I present some numerical examples that include synthetic data and Marmousi data. In these examples, I used Kirchhoff prestack depth migration. The layer-stripping procedure for velocity analysis can be stated as follows:

Begin from the first block.—

- 1) estimate velocity parameters iteratively
 - (a) migrate with an initial guess of velocity;
 - (b) sort the migrated data into common image gathers;
 - (c) measure imaged depths and evaluate the derivative function;
 - (d) update velocity by using the perturbation formula;
- 2) image velocity interface by using corrected velocity

Repeat steps 1 and 2 for next block.—When velocity and velocity gradients are estimated simultaneously in one block, the iteration tends to be unstable, as explained in the previous section. To overcome this difficulty, it is preferable to estimate velocity first. This estimation will yield an averaged velocity and give a better initial guess for the velocity distribution in this block.

Simple synthetic data

The first example is synthetic data generated by the Kirchhoff integral. The velocity model shown in Figure 3 consists of six blocks. The velocity function in each block is constant or linear. Synthetic seismic traces are generated from this model, with five offsets ranging from 100 m to 900 m.

The velocity analysis process is outlined as follows:

In the first layer, the initial guess of velocity is 1500 m/s, with an error of 30%. Structural images are distorted in the

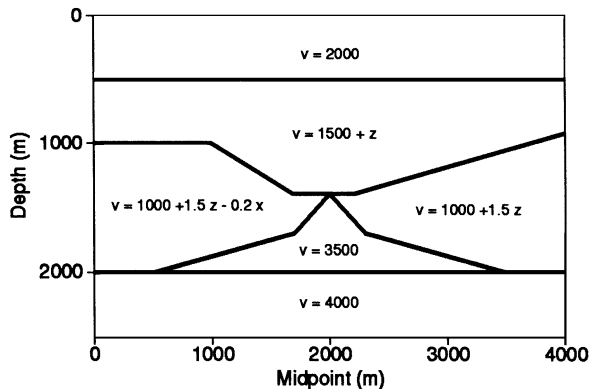


FIG. 3. The true velocity model. The velocity unit is m/s.

migrated data using this erroneous velocity, shown in Figure 4. Two common-image gathers of the migrated data also indicate that the initial guess is incorrect, shown in Figure 5. The imaged depths are measured at these two image locations for velocity updating. After two iterations, the corrected velocity is 2004 m/s, while the true value is 2000 m/s.

In the second layer, there are two parameters used in the velocity distribution: a constant velocity and a vertical constant gradient. The initial guess takes 2004 m/s that is the estimated velocity in the first layer. If this initial velocity is used directly to estimate the velocity constant and vertical gradient, the iteration will be divergent. Therefore, I only estimated the velocity constant in the first step. The updated velocity is 2420 m/s and gives a better approximation to the true velocity. In the second iteration, the two parameters of velocity function are updated simultaneously. The corrected velocity function is

$$v(z) = 1480 + 1.01z \text{ m/s.}$$

The true velocity function is $v(z) = 1500 + 1.0z \text{ m/s}$.

The final velocity model estimated through velocity analysis is shown in Figure 6. Flat residual moveouts at common-image gathers, shown in Figure 7, indicate correctness of the estimated velocity. With this velocity model, migration is implemented and the structural image is shown in Figure 8, which is close to the true subsurface model as shown in Figure 3.

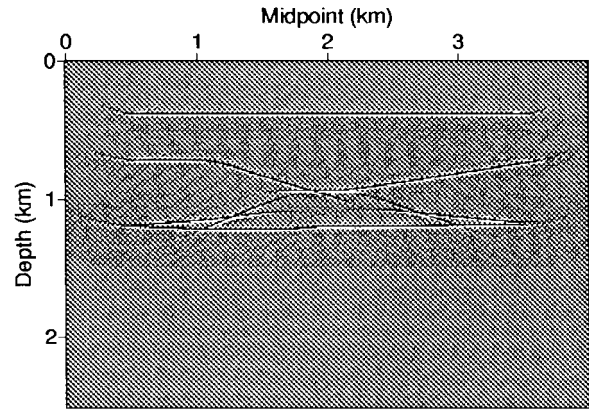


FIG. 4. Prestack migration with the initial constant velocity. The offset is 100 m.

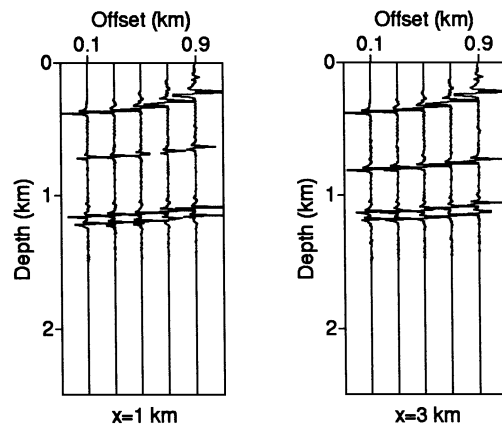


FIG. 5. Two common-image gathers from the migrated data with the initial velocity.

Also, I test the computation of g_1 in the first layer. The numerical g_1 is computed from the ratio of the amplitudes in the Kirchhoff migration outputs; then I compare the numerical g_1 with the true value calculated in equation (36). In this test, $v_0 = 500$ m/s and $d = 0$. The result listed in Table 1 shows that the numerical value of g_1 is accurate for all offsets. This validates the estimation technique based on the stationary phase principle.

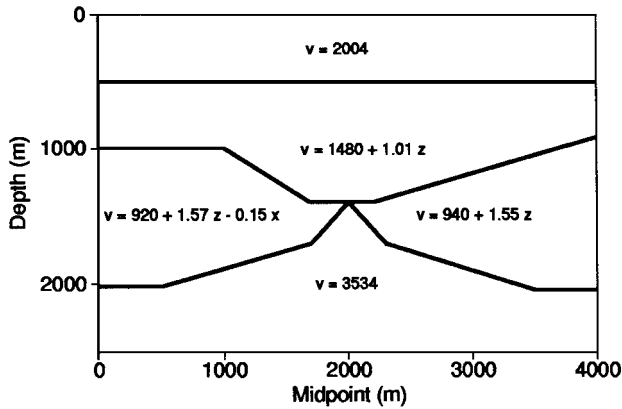


FIG. 6. Final estimated model from velocity analysis.

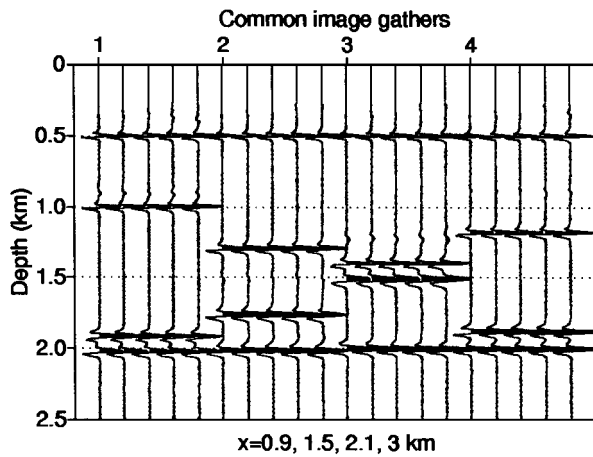


FIG. 7. Common-image gathers from the migrated data with the velocity in Figure 6.

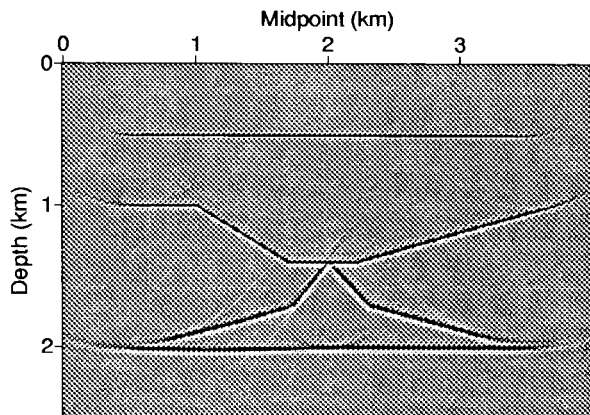


FIG. 8. Migration with the estimated velocity model in Figure 6.

Marmousi data

The Marmousi data set is generated by using a 2-D acoustic finite-difference modeling program. The model contains many reflectors, steep dips, and strong velocity variations both in lateral and vertical directions (with a minimum velocity of 1500 m/s and a maximum velocity of 5500 m/s), shown in Figure 9. The data set consists of 240 shots with 96 traces per shot. The initial offset is 200 m; both the shot and the receiver spacings are 25 m. The first shot is at the lateral position 3000 m. Here nineteen common-offset data gathers are used for velocity analysis. The selected offsets range from 200 m to 2000 m with a spacing 100 m.

During the velocity analysis process, I assume that the velocity field is a macro model and that the velocity distribution is a linear function in each block. Velocity analysis results surely depend on what kind of migration algorithm is used. For a velocity model complicated as the Marmousi, migration based on the first arrivals fails to correctly image complicated structures when multiple arrivals exist (Geoltrain and Brac, 1993). Here, a paraxial ray-tracing algorithm is used to implement Kirchhoff migration. In this approach, the traveltimes corresponding to the maximum energy is chosen when multiple arrivals exist.

Using the Kirchhoff migration algorithm by paraxial ray tracing, velocity analysis is done through the central bottom parts of the Marmousi model. The updated velocity model, shown in Figure 10, consists of 19 blocks. In each block, the velocity distribution is a constant or linear function of the depth. Comparison of the estimated velocity model to the true one at three lateral locations is shown in Figure 11. One can see that the estimated velocity matches the true model well, except for thin layers. In fact, from the sensitivity analysis, velocities in these thin layers cannot be determined well. The stacked migration section using the velocity model in Figure 10 is shown in Figure 12. Compared to the migration result using the true velocity model, shown in Figure 13, Figure 12 gives an acceptable structural image even in the central bottom parts, which indicates the capability of this migration velocity analysis approach for handling complex structures. The subsurfaces are well imaged except for some detailed features in the central bottom parts. Some blurry imaging in the central bottom parts may be caused by missing high velocity zones. Figure 9 shows that the real velocity contains several small high-velocity zones in the central parts. These high-velocity zones do not appear in Figure 10 because of the limitations of velocity analysis and the resolution of migration imaging.

Selected common image gathers from migrated data using the estimated model are shown in Figures 14, 15, and 16 which represent the left, central, and right parts of the model, respectively. Flat residual moveouts in Figures 14, 16, and the upper part of Figure 15 indicate the correctness of the estimated

Table 1. Test for derivative function g_1 as defined by equation (15). The unit of offset and depth is m.

| Offset (m) | Imaged depth (m) | Numerical g_1 | True g_1 |
|------------|------------------|-----------------|------------|
| 100 | 370 | 0.249 | 0.251 |
| 300 | 360 | 0.278 | 0.282 |
| 500 | 330 | 0.345 | 0.346 |
| 700 | 290 | 0.476 | 0.475 |
| 900 | 210 | 0.773 | 0.783 |

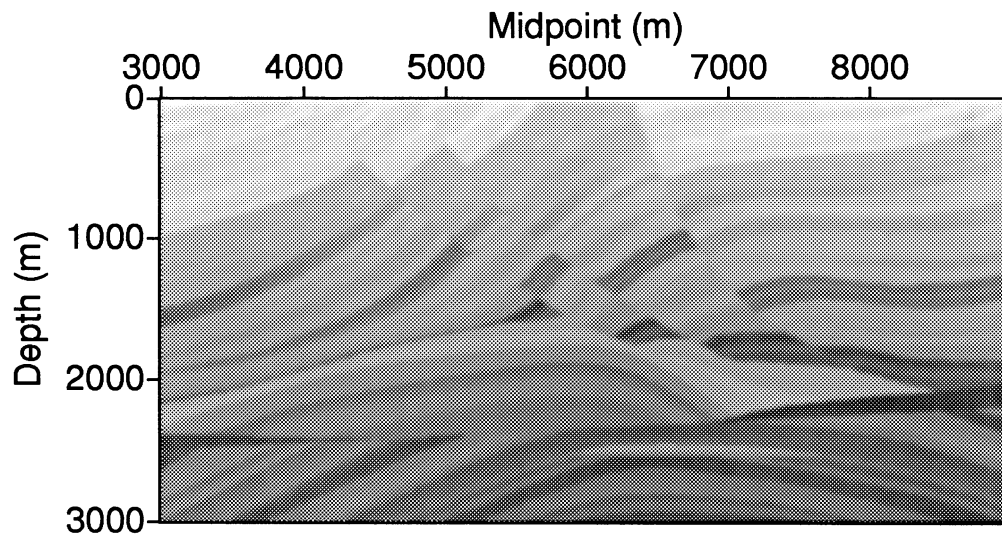


FIG. 9. The Marmousi velocity model. The darker shading denotes higher velocity.

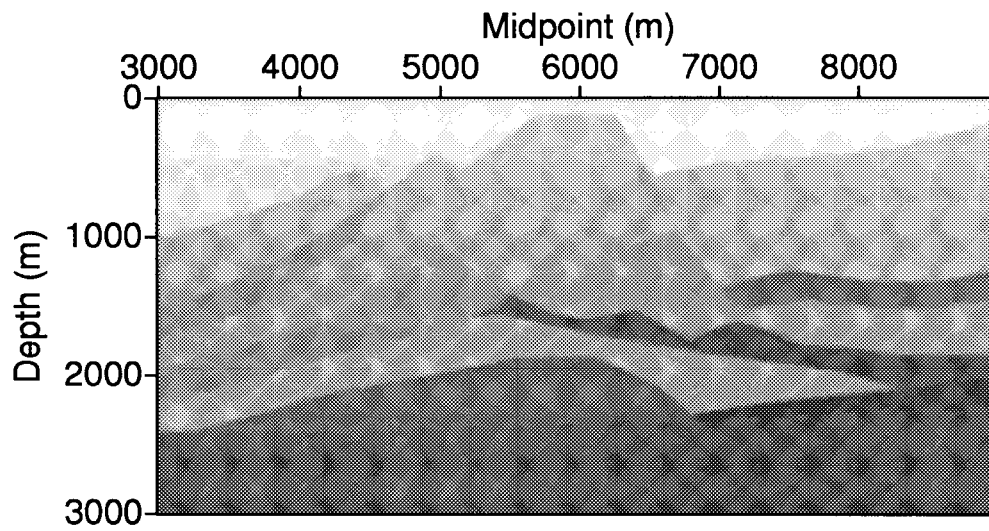


FIG. 10. The estimated Marmousi velocity model.

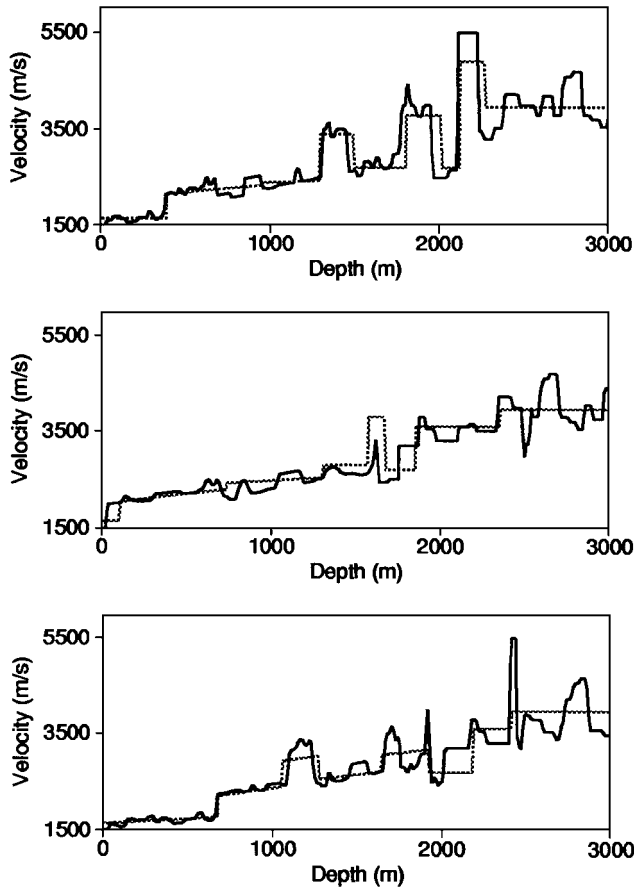


FIG. 11. Comparison of the true velocity model to the estimated one. The dark curve denotes the true velocity and the gray denotes the estimated velocity. The top figure is at location $x = 8$ km; the middle, at location $x = 6$ km; the bottom, at location $x = 4$ km.

velocity in these areas. The bottom part of Figure 15 shows incoherent signals that affect the accuracy of velocity estimation in this particular area. Notice that, at the same common image gathers (see Figure 17), migrated data using the true velocity also contain obvious incoherency in residual moveouts, although the stacked section shows a good image. This example demonstrates that for an extremely complex structure it is very difficult to identify the correct velocity model based on the criterion of kinematic coherence.

CONCLUSIONS

Imaging complex structures (such as the Marmousi data) requires powerful prestack depth-migration algorithms, as well as advanced velocity analysis techniques. The velocity analysis method in this paper provides a useful tool for updating a velocity model by matching a criterion based on prestack information, which is one of the key elements in velocity model determination (Versteeg, 1994). To obtain a more satisfactory velocity analysis result for a complicated model, as Versteeg concluded, one also needs related geologic information as constraints.

ACKNOWLEDGMENTS

I sincerely thank Dr. Norman Bleistein for all the help and guidance he has given me. This research is supported by the members of the Consortium Projection on Seismic Inverse Methods for Complex Structures at the Center for Wave Phenomena, Colorado School of Mines. This work is also partially supported by the Office of Naval Research Applied Analysis Program, Grant no. N00014-91-J-1267.

REFERENCES

- Al-Yahya, K., 1989, Velocity analysis by iterative profile migration: *Geophysics*, **54**, 718-729.
- Bleistein, N., Cohen, J., and Hagin, F., 1987, Two and one-half dimensional Born inversion with an arbitrary reference: *Geophysics*, **52**, 26-36.

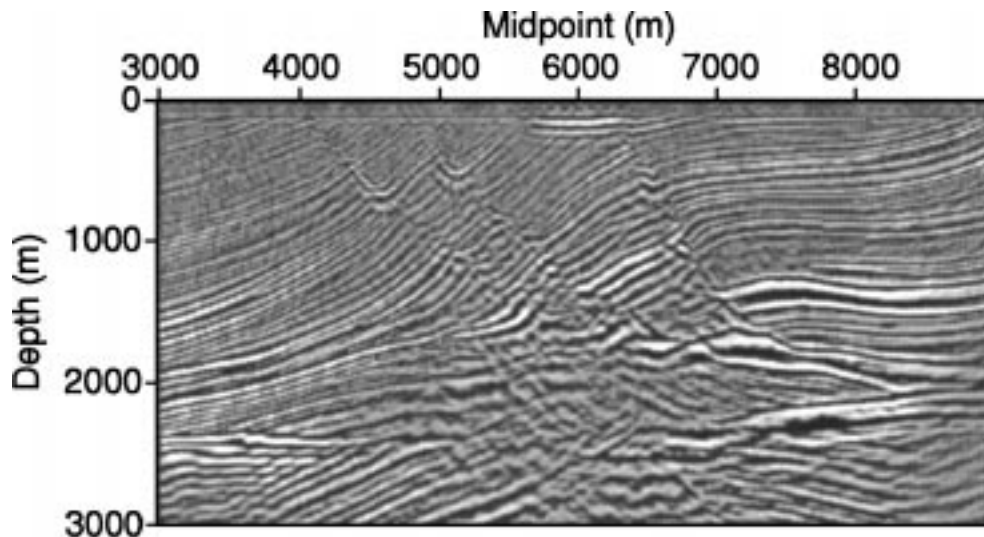


FIG. 12. Nineteen-offset stacked migration output for the Marmousi data. The input velocity is one in Figure 10.

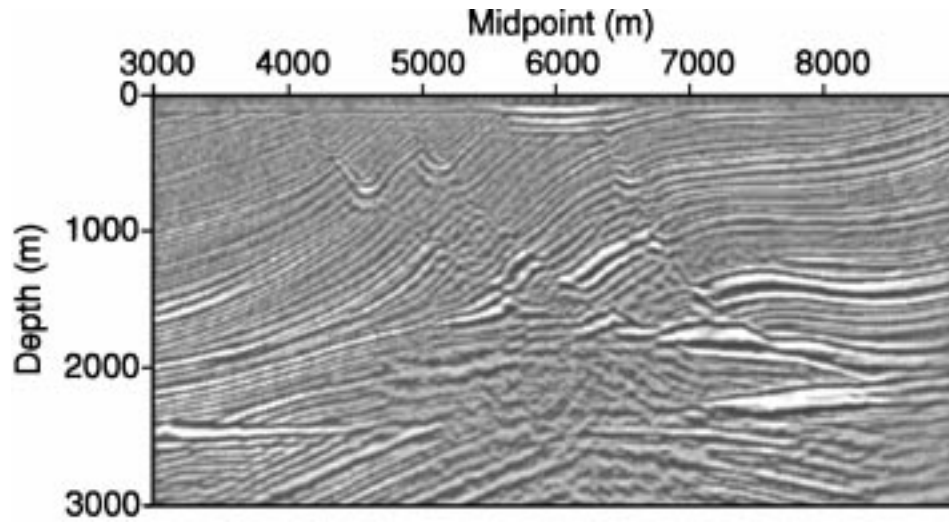


FIG. 13. Nineteen-offset stacked migration output for the Marmousi data. The true velocity is used.

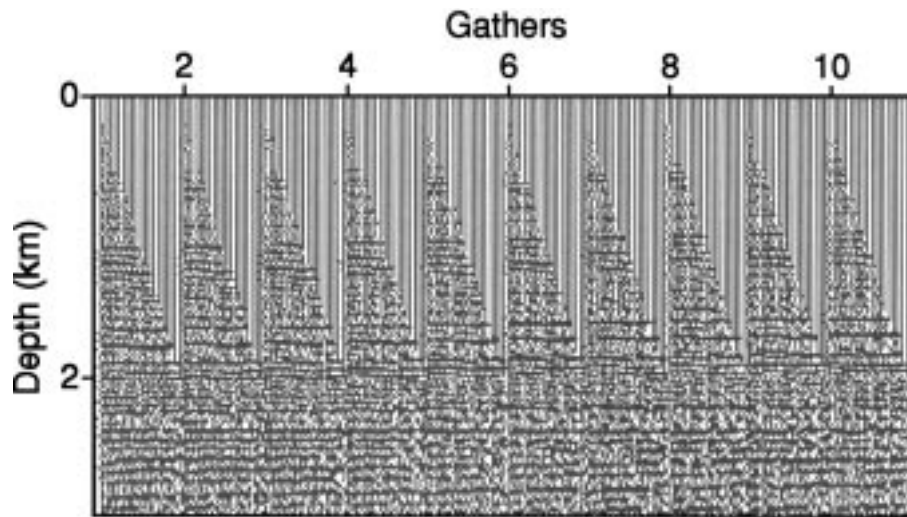


FIG. 14. Ten common-image gathers. Nineteen offsets in each CIG. The image location ranges from 4 km to 4.25 km.

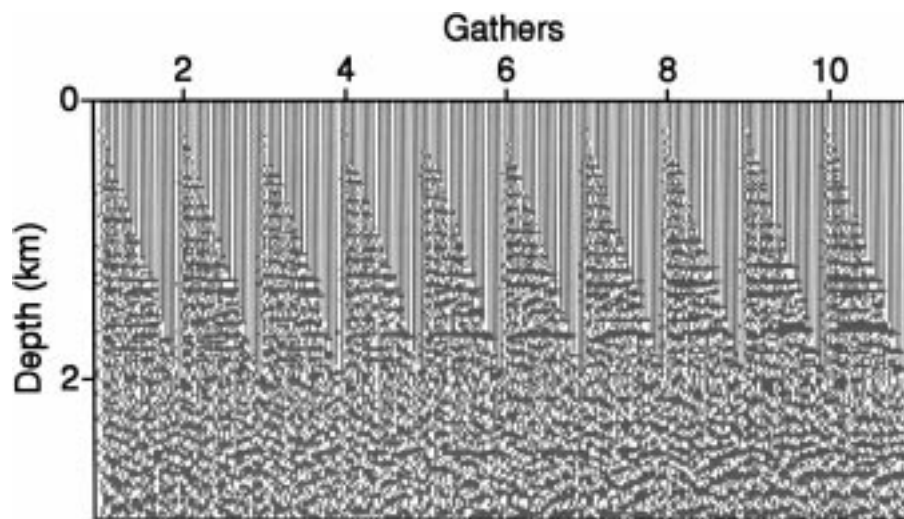


FIG. 15. Ten common-image gathers. Nineteen offsets in each CIG. The image location ranges from 6 km to 6.25 km.

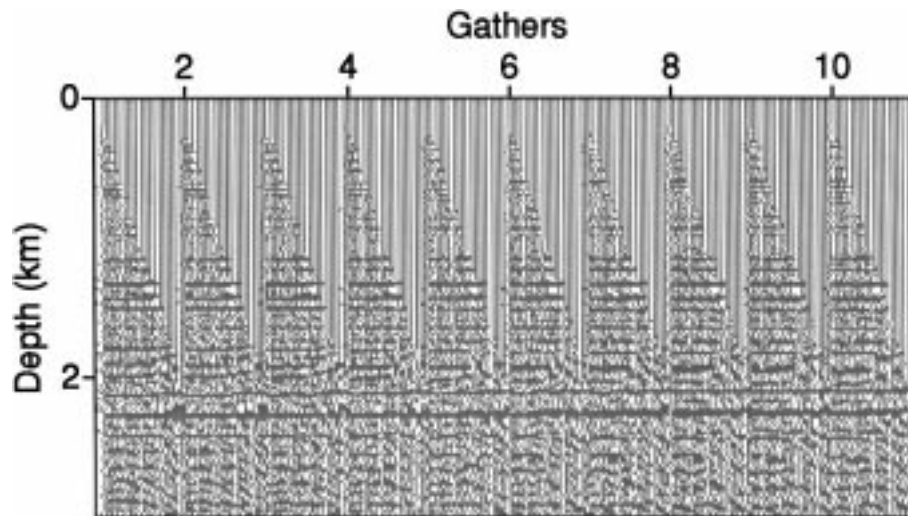


FIG. 16. Ten common-image gathers. Nineteen offsets in each CIG. The image location ranges from 8 km to 8.25 km.

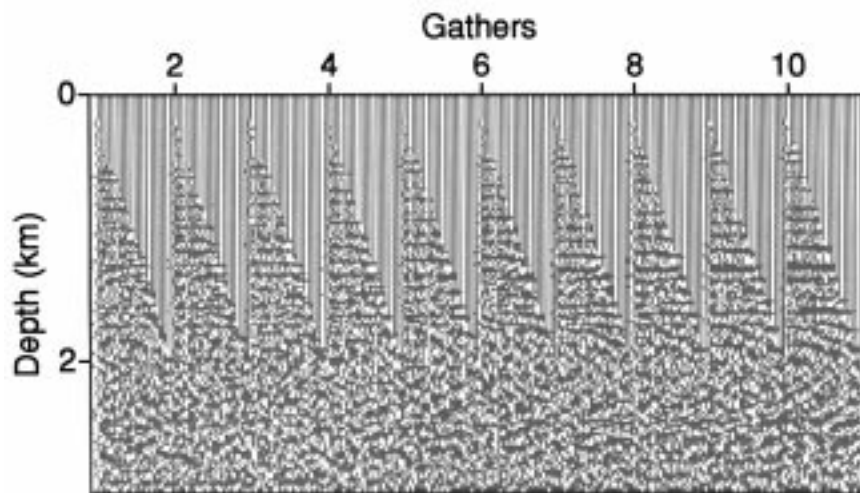


FIG. 17. Ten common-image gathers from migrated data using the true velocity. The image location ranges from 6 km to 6.25 km.

- Deregowski, S. M., 1990, Common-offset migrations and velocity analysis: *First Break*, **8**, No. 6, 225–234.
- Geoltrain, S., and Brac, J., 1993, Can we image complex structures with first-arrival traveltimes migration: *Geophysics*, **58**, 564–575.
- Lafond, C. F., and Levander, A. R., 1993, Migration moveout analysis and depth focusing: *Geophysics*, **58**, 91–100.
- Lee, W., and Zhang, L., 1992, Residual shot profile migration: *Geophysics*, **57**, 815–822.
- Liu, Z., and Bleistein, N., 1992, Velocity analysis by residual moveout: 62nd Ann. Internat. Mtg., Soc. Expl. Geophys., Expanded Abstracts, 1034–1036.

- Liu, Z., and Bleistein, N., 1995, Migration velocity analysis: Theory and an iterative algorithm: *Geophysics*, **60**, 142–153.
- MacKay, S., and Abma, R., 1992, Imaging and velocity estimation with depth-focusing analysis: *Geophysics*, **57**, 1608–1622.
- Stork, C., and Clayton, R. W., 1991, An implementation of tomographic velocity analysis: *Geophysics*, **56**, 472–482.
- Toldi, J., 1989, Velocity analysis without picking: *Geophysics*, **54**, 191–199.
- Versteeg, R., 1994, The Marmousi experience: velocity model determination on a synthetic complex data set: *The Leading Edge*, **13**, No. 927–936.

APPENDIX A

EQUATION SYSTEM FOR PERTURBATION

In this Appendix, a linear equation system is derived for parameter estimation in the perturbation method.

By using the matrix and vector notations in equation (24), I obtain

$$\begin{aligned}\overline{\delta\hat{z}^{(k)}} &= \frac{1}{m} \sum_{j=1}^m \delta z_j^{(k)} \\ &= \frac{1}{m} \sum_{j=1}^m \sum_{i=1}^n g_{ij}^{(k)} \delta\lambda_i \\ &= \sum_{i=1}^n \left(\delta\lambda_i \frac{1}{m} \sum_{j=1}^m g_{ij}^{(k)} \right) \\ &= \sum_{i=1}^n \left(\delta\lambda_i \overline{\hat{g}_i^{(k)}} \right),\end{aligned}\quad (\text{A-1})$$

and

$$\begin{aligned}z_j^{(k)} + \delta z_j^{(k)} - \overline{\hat{z}^{(k)}} + \overline{\delta\hat{z}^{(k)}} &= z_j^{(k)} - \overline{\hat{z}^{(k)}} + \delta z_j^{(k)} - \overline{\delta\hat{z}^{(k)}} \\ &= z_j^{(k)} - \overline{\hat{z}^{(k)}} + \sum_{i=1}^n \delta\lambda_i \left(g_{ij}^{(k)} - \overline{\hat{g}_i^{(k)}} \right).\end{aligned}\quad (\text{A-2})$$

Define a quadratic objective function

$$f(\delta\hat{\lambda}) \equiv \sum_{k=1}^K \sum_{j=1}^m \left(z_j^{(k)} + \delta z_j^{(k)} - \overline{\hat{z}^{(k)}} + \overline{\delta\hat{z}^{(k)}} \right)^2. \quad (\text{A-3})$$

Thus, finding the minimum of $f(\delta\hat{\lambda})$ is equivalent to setting its gradient with respect to $\delta\hat{\lambda}$ equal $\hat{0}$, i.e.,

$$\frac{\partial f(\delta\hat{\lambda})}{\partial \delta\lambda_\ell} = 0 \quad \ell = 1, 2, \dots, n. \quad (\text{A-4})$$

APPENDIX B

DERIVATIVE FUNCTIONS IN A SIMPLE CASE

In this Appendix, the representation for derivatives of imaged depths with respect to velocity and velocity vertical gradient is derived for a horizontal reflector and a constant background velocity.

From equation (32),

$$\frac{\partial \tau}{\partial \lambda} = \int_L \frac{\partial}{\partial \lambda} \left(\frac{1}{v(x, z)} \right) dL = - \int_L v^{-2}(x, z) \frac{\partial v(x, z)}{\partial \lambda} dL, \quad (\text{B-1})$$

where L is the raypath. Here, to simplify notation, I suppose that all derivatives with respect to λ are evaluated at $\lambda_1 = \lambda_2 = 0$. When the background velocity is a constant v_0 as in equation (34), equation (B-1) becomes

$$\frac{\partial \tau}{\partial \lambda} = - \frac{1}{\cos \theta} \int_0^z v_0^{-2} \frac{\partial v(x, z')}{\partial \lambda} dz', \quad (\text{B-2})$$

where θ is the angle between the raypath and the vertical. For the velocity function in equation (35), if $z > d$, then

$$\frac{\partial v(x, z)}{\partial \lambda_1} = 1, \quad \frac{\partial v(x, z)}{\partial \lambda_2} = z - z_0; \quad (\text{B-3})$$

if $z < d$, then

$$\frac{\partial v(x, z)}{\partial \lambda_1} = \frac{\partial v(x, z)}{\partial \lambda_2} = 0. \quad (\text{B-4})$$

By using equation (A-2),

$$f(\delta\hat{\lambda}) = \sum_{k=1}^K \sum_{j=1}^m \left[z_j^{(k)} - \overline{\hat{z}^{(k)}} + \sum_{i=1}^n \delta\lambda_i \left(g_{ij}^{(k)} - \overline{\hat{g}_i^{(k)}} \right) \right]^2. \quad (\text{A-5})$$

The derivatives computed from this function are

$$\begin{aligned}\frac{\partial f(\delta\hat{\lambda})}{\partial \delta\lambda_\ell} &= 2 \sum_{k=1}^K \sum_{j=1}^m \left[z_j^{(k)} - \overline{\hat{z}^{(k)}} \right. \\ &\quad \left. + \sum_{i=1}^n \delta\lambda_i \left(g_{ij}^{(k)} - \overline{\hat{g}_i^{(k)}} \right) \right] \left(g_{\ell j}^{(k)} - \overline{\hat{g}_\ell^{(k)}} \right), \\ &= 2 \sum_{k=1}^K \sum_{j=1}^m \left(z_j^{(k)} - \overline{\hat{z}^{(k)}} \right) \left(g_{\ell j}^{(k)} - \overline{\hat{g}_\ell^{(k)}} \right), \\ &\quad + 2 \sum_{k=1}^K \sum_{j=1}^m \sum_{i=1}^n \delta\lambda_i \left(g_{ij}^{(k)} - \overline{\hat{g}_i^{(k)}} \right) \left(g_{\ell j}^{(k)} - \overline{\hat{g}_\ell^{(k)}} \right), \\ &= 2 \left[\sum_{k=1}^K A^{(k)} \right] \delta\hat{\lambda} + 2 \sum_{k=1}^K \hat{b}^{(k)},\end{aligned}\quad (\text{A-6})$$

where the notations in equation (24) are used. The condition (A-4) implies that

$$\left[\sum_{k=1}^K A^{(k)} \right] \delta\hat{\lambda} = - \sum_{k=1}^K \hat{b}^{(k)}. \quad (\text{A-7})$$

This completes the verification that the solution of equation (28) achieves the minimum of variance (20).

Therefore,

$$\frac{\partial \tau}{\partial \lambda_1} = - \frac{1}{\cos \theta} \int_d^z \frac{1}{v_0^2} dz' = - \frac{1}{\cos \theta} \frac{z - d}{v_0^2}, \quad (\text{B-5})$$

and

$$\begin{aligned}\frac{\partial \tau}{\partial \lambda_2} &= - \frac{1}{\cos \theta} \int_d^z \frac{z' - z_0}{v_0^2} dz' \\ &= - \frac{1}{\cos \theta} \frac{(z - z_0)^2 - (d - z_0)^2}{2v_0^2}.\end{aligned}\quad (\text{B-6})$$

Because the reflector is horizontal, the raypaths from the source and the receiver are symmetric. I obtain

$$\cos \theta_s = \cos \theta_r = \frac{z}{\sqrt{z^2 + h^2}}. \quad (\text{B-7})$$

Substituting equations (B-7), (B-5), and (B-6) into equation (15) yields

$$g_1(x, h) = \frac{h^2 + z^2}{z^2} \frac{z - d}{v_0}, \quad (\text{B-8})$$

and

$$g_2(x, h) = \frac{h^2 + z^2}{z^2} \frac{(z - z_0)^2 - (d - z_0)^2}{2v_0}. \quad (\text{B-9})$$

This completes the verification of equations (36) and (37).